Computer Coupling of Phase Diagrams and Thermochemistry 32 (2008) 669–674

Contents lists available at ScienceDirect

Computer Coupling of Phase Diagrams and Thermochemistry

journal homepage: www.elsevier.com/locate/calphad

Thermodynamic analysis for the size-dependence of $Si_{1-x}Ge_x$ nanowire composition grown by a vapor–liquid–solid method

Inyoung Sa, Byeong-Moon Lee, Cheol-Joo Kim, Moon-Ho Jo, Byeong-Joo Lee *

Department of Materials Science and Engineering, Pohang University of Science and Technology, Pohang 790-784, Republic of Korea

ARTICLE INFO

Article history:
Received 4 July 2008
Received in revised form
16 September 2008
Accepted 16 September 2008
Available online 7 October 2008

Keywords:
Thermodynamics
Alloy nanowire
Si–Ge
Capillarity effect
VLS method

ABSTRACT

A fundamental thermodynamic approach for the size dependence of the $Si_{1-x}Ge_x$ alloy nanowire composition grown by a vapor–liquid–solid method is proposed. It is shown that the experimentally observed size dependence of the $Si_{1-x}Ge_x$ alloy nanowire composition originates from the capillarity effect. The direct effect of the capillarity on the composition of liquid droplets is clarified and rationalized based on the solution thermodynamics. The present approach can be a starting point for more sophisticated and quantitative studies to predict and control the composition of alloy nanowires synthesized by similar methods.

1. Introduction

$Si_{1-x}Ge_x$ nanowires have received a great deal of attention due to their promising enhancement in optoelectronics [1,2], sensing and field emission [3,4], etc. A precise control of the chemical composition in $Si_{1-x}Ge_x$ nanowires, which determines its electronic characteristics, has been regarded as a critical factor for advanced device performance. The effect of various process conditions on the composition of $Si_{1-x}Ge_x$ nanowires has been investigated using various synthetic techniques, such as laser-assisted catalytic growth (LCG) [5], chemical vapor deposition (CVD) [6], molecular beam epitaxy (MBE) [7], and vapor–liquid–solid (VLS) method [8–10]. It has been shown [8–10] that $Si_{1-x}Ge_x$ nanowires can be grown in the entire composition range by controlling the $GeH_4/(GeH_4 + SiH_4)$ inlet gas flow ratio and the growth temperature.

However, in addition to the process condition, it was found that the wire size (diameter) can also have an effect on the wire composition under a single process condition [10]. This size dependence of wire composition was first observed by Yang et al. [10] who claimed a decreasing Ge fraction with decreasing nanowire diameter in a range of 5–50 nm, and was confirmed by Zhang et al. [11] who performed a thorough experimental work. Some time ago, a size dependence of the growth rate of VLS grown pure component whiskers had been observed and explained in terms of the Gibbs–Thompson effect [12]. Based on the size dependence of growth rate of nanowires [12] and assuming that the alloy wire composition is determined by the relative growth rate of individual pure component nanowires [9], Zhang et al. [11] also proposed an empirical model to predict the wire composition. In this approach, the model parameters were determined by fitting to experimental data. Even though the growth rate was formulated considering the Gibbs–Thompson effect and a good agreement was obtained between the model prediction and experimental data, because of the empirical fitting, the result cannot be regarded to indicate that the Gibbs–Thompson effect causes the size dependence of wire composition. Also, as mentioned by the authors [11], a more fundamental understanding of the size effect is necessary for a precise control of the nanowire composition.

In the present study, we provide a fundamental thermodynamic analysis to confirm that the size dependence of alloy nanowire composition grown by a VLS method indeed originates from the Gibbs–Thompson effect on the thermodynamics of the Au droplet catalyst and the $Si_{1-x}Ge_x$ nanowire. The results will be rationalized by analyzing direct effect of the capillarity on the liquid droplet composition based on solution thermodynamics.

2. Thermodynamic approach

The VLS method is a process for growing nano wires where a liquid metal droplet or catalyst (initially pure Au, in the present case) acts as a energetically favored site for absorption of gas-phase reactants, supersaturates and grows a 1D structure (wire) of the

* Corresponding author. Tel.: +82 54 2792157; fax: +82 54 2792399.
E-mail address: calphad@postech.ac.kr (B.-J. Lee).

0364-5916/$ – see front matter © 2008 Elsevier Ltd. All rights reserved.
doi:10.1016/j.calphad.2008.09.011

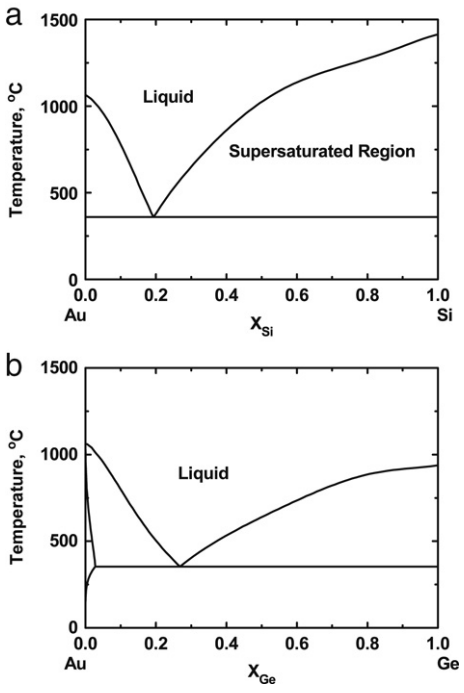

Fig. 1. Calculated phase diagrams of the (a) Au–Si and (b) Au–Ge binary systems.

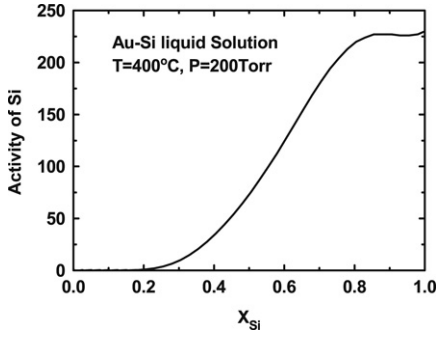

Fig. 2. Calculated activity of Si in the Au–Si liquid alloys at 400 °C and 200 Torr. The reference state of Si is the solid diamond structure.

materials. The present authors view the VLS growth of nanowires to be composed of two interfacial reactions. One is the reaction between vapor and liquid droplets on the surface of the liquid droplet. The other is the reaction between liquid droplets and solid nanowires on the interface between the two. The vapor can be regarded to be composed of the initial SiH_4 and/or GeH_4, H_2 gases and decomposed Si and/or Ge atoms. The incorporation of Si and/or Ge atoms into the initially solid Au nano particles results in the formation of liquid Si(Ge)–Au alloy droplets even though the process temperature (around 400 °C) is well below the melting point of pure Au. This can be rationalized from the phase diagram of the Au–Si or Au–Ge binary system which is characterized by the presence of a deep eutectic point (see the Au–Si phase diagram in Fig. 1, for example). The formation and growth of the Si–Ge solid phase (nanowires) indicates that the composition of the liquid droplet would correspond to a supersaturated region designated in Fig. 1. The composition of the $Si_{1-x}Ge_x$ nanowire can be estimated by calculating phase equilibria between the liquid and solid phases taking the supersaturated liquid composition as the overall composition.

The issue now is how to estimate the composition of the liquid droplet for various process conditions (temperature and flow rates of SiH_4 and/or GeH_4 and H_2 gases). Fig. 2 shows how the activity of Si changes with the liquid composition at 400 °C, for example. If a local equilibrium between the vapor and liquid phases can be assumed on the liquid surface, the liquid composition can be estimated from the equilibrium activity of Si and/or Ge in the vapor phase. The equilibrium activity values of Si and/or Ge in vapor can be easily obtained from thermodynamic calculation because the Gibbs energy of formation of SiH_4 and/or GeH_4 is readily available in thermodynamic data handbooks. For a given process condition (temperature and flow rates), the thermodynamic state (activities of individual components) of the vapor phase would be fixed and uniform on the surface of substrate. From the thermodynamic state of vapor and the assumed local equilibrium between the vapor and liquid, the composition of the supersaturated liquid and then the composition of solid nanowire can be estimated. The key idea of the present approach is that under the same thermodynamic state of the vapor phase, the resultant compositions of liquid and solid phases would be dependent on the droplet and wire diameter if the size effect is considered during the thermodynamic calculation. The size effect can be considered by including the following Gibbs–Thompson equation in the molar Gibbs free energy expressions for the liquid and solid phases:

$$\Delta G_{G-T} = \alpha \frac{\gamma}{r} V_m, \tag{1}$$

where r is the radius, γ is the surface energy and V_m is the molar volume. α is a geometrical factor which is 1 for cylindrical (wire) and 2 for spherical (droplet) materials.

In the present study, the above mentioned thermodynamic calculations were performed for $Si_{1-x}Ge_x$ nanowires with various diameters. The solid nanowire was treated as a Si–Ge binary solid solution phase and the liquid droplet was treated as a Si–Ge-Au ternary liquid solution phase. The size of the solid nanowire was assumed to be the same as that of the liquid droplet in individual wires. The point here was to see if relatively low Ge content is indeed predicted for thin wires under a given (fixed) process condition and to find governing process factors that have a decisive effect on the size dependence of wire composition. For thermodynamic calculations, the ThermoCalc software [13] and SGTE solution and pure substance databases [14] which are based on the CALPHAD method [15] were used. All calculations were carried out for a pressure of 200 Torr and temperature of 400 °C, which is the experimental condition of Yang et al. [10].

In order to estimate the supersaturated liquid composition, an attempt was made to calculate the equilibrium chemical activities of Si and Ge for a typical process condition [10] (total pressure, temperature and ratio between SiH_4, GeH_4 and H_2 gases). Unexpectedly, the calculated equilibrium activities (or partial pressures) of Si and Ge in the vapor phase for the given condition were much higher than the values in Fig. 2 by several orders of magnitude. This meant that the vapor phase would never reach an equilibrium state and the local equilibrium between the vapor and liquid droplets on the liquid surface could not be assumed. It was impossible to estimate the supersaturated liquid composition from the equilibrium calculation on the vapor phase.

As a means to overcome this difficulty, in the present study, a supersaturated initial liquid composition was assigned and an imaginary vapor phase which is in equilibrium with the liquid was assumed. Then, activities of Si and Ge in the vapor phase which will result in the assigned liquid composition for bulk liquid (without considering the Gibbs–Thompson effect) were calculated. Assuming a local equilibrium between the imaginary vapor and liquid phases, the liquid composition was calculated again, but now considering the Gibbs–Thompson effect. The calculated liquid composition was different from the initially assigned one. The newly calculated liquid composition was regarded as the supersaturated composition of the liquid droplet,

Table 1
Surface energy and molar volume of individual elements [19–21], and thermodynamic model and parameters [14] for the Au–Si–Ge liquid alloy

Phase	Element	Surface energy (J/m^2)	Molar volume (m^3/mol)
Liquid	Au	$\gamma^l_{Au} = 1.169 - 0.00025(T - 1336.15)$	$V^l_{Au} = 11.3 \times 10^{-6} \cdot [1.0 + 0.000069(T - 1336.15)]$
	Si	$\gamma^l_{Si} = 0.865 - 0.00013(T - 1687.15)$	$V^l_{Si} = 11.1 \times 10^{-6} \cdot [1.0 + 0.000014(T - 1687.15)]$
	Ge	$\gamma^l_{Ge} = 0.621 - 0.00026(T - 1231.65)$	$V^l_{Ge} = 13.2 \times 10^{-6} \cdot [1.0 + 0.0000089(T - 1231.65)]$
Solid	Au	$\gamma^s_{Au} = 1.626 - 0.0002705(T - 298.2)$	$V^s_{Au} = 1.021 \times 10^{-5}$
	Si	$\gamma^s_{Si} = 1.107 - 0.0001589(T - 298.2)$	$V^s_{Si} = 1.206 \times 10^{-5}$
	Ge	$\gamma^s_{Ge} = 0.760 - 0.0002531(T - 298.2)$	$V^s_{Ge} = 1.365 \times 10^{-5}$

$G^{liq}_m = x_{Au}\,{}^oG^{liq}_{Au} + x_{Si}\,{}^oG^{liq}_{Si} + x_{Ge}\,{}^oG^{liq}_{Ge} + RT(x_{Au}\ln x_{Au} + x_{Si}\ln x_{Si} + x_{Ge}\ln x_{Ge}) + x_{Au}x_{Si}L_{Au,Si} + x_{Au}x_{Ge}L_{Au,Ge} + x_{Si}x_{Ge}L_{Si,Ge}$

${}^oG^{liq}_{Au} = +12552 - 9.38411T + {}^oG^{sol}_{Au}$
${}^oG^{liq}_{Si} = +50696 - 30.0994T + 2.09307 \times 10^{-21}T^7 + {}^oG^{sol}_{Si}$
${}^oG^{liq}_{Ge} = 37142 - 30.6846T + 8.5676110^{-21}\,T^7 + {}^oG^{sol}_{Ge}$
$L_{Au,Si} = -23864 - 16.2344T + (x_{Au} - x_{Si})(-20530 - 6.0396T) + (x_{Au} - x_{Si})^2(-8171 - 4.2732T) + (x_{Au} - x_{Si})^3(-33138 + 26.5667T)$
$L_{Au,Ge} = -18060 - 13.0854T + (x_{Au} - x_{Ge})(-6132 - 9.1018T) + (x_{Au} - x_{GE})^2(-4734 - 3.2591T) + (x_{Au} - x_{Ge})^3(-8121 - 5.8254T)$
$L_{Si,Ge} = 0$

The solid Si–Ge alloy was assumed as an ideal solution.

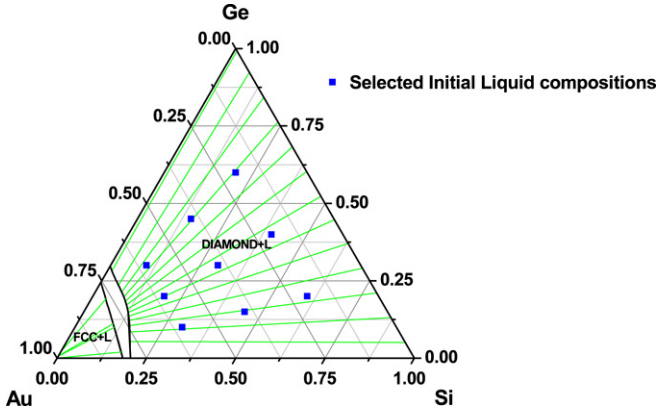

Fig. 3. Calculated phase diagram of the Au–Si–Ge ternary system at 400 °C, and selected compositions of initial supersaturated bulk liquid alloys used as the starting point of the present thermodynamic approach.

and was used as the overall composition to calculate the solid wire composition. Several initial liquid compositions were selected in the supersaturated composition range and are designated in Fig. 3. This approach cannot be used to predict the liquid droplet composition from the real process condition, but certainly can be used to examine the size effect on the final wire composition under a given, specific process condition without losing the physical significance.

For the evaluation of the Gibbs–Thompson effect given in Eq. (1), numeric values for the molar volume and surface energy of liquid and solid alloys had to be provided. Those quantities for individual elements were available from the literature as listed in Table 1, together with the thermodynamic model and model parameters used for the liquid. The relationship between size and surface energy is still controversial, but it is known that the drastic change of surface energy appears only below a few nanometer. [16, 17] In the present diameter range of 5–150 nm, the surface energy for nano particles or wires were assumed to be independent from the size and be the same as bulk properties. The same assumption was made also for the molar volume of nano particles or wires. No predicative relation between the molar volume of alloys and that of individual elements is known. The simplest way was to apply the rule of mixture. For the liquid, the molar volume of each alloy was estimated from the rule of mixture based on the initial composition as follows:

$$\overline{V^l} = x^{ini}_{Au} \cdot V^l_{Au} + x^{ini}_{Si} \cdot V^l_{Si} + x^{ini}_{Ge} \cdot V^l_{Ge}, \quad (2)$$

where V_i are molar volume of pure elements taken from Table 1 and x_i are mole fraction of individual elements in the initial liquid composition. Once the value of an initial molar volume is determined using Eq. (2), it was further assumed to be constant during the whole calculation for the convenience of equilibrium calculation. The same assumption was made for the molar volume of the solid phase. Because the solid nanowire was treated as a Si–Ge binary solid solution, the rule of mixture was applied only between Si and Ge, again based on the initial liquid composition, as follows:

$$\overline{V^s} = \frac{x^{ini}_{Si} \cdot V^s_{Si} + x^{ini}_{Ge} \cdot V^s_{Ge}}{x^{ini}_{Si} + x^{ini}_{Ge}}. \quad (3)$$

The molar volume data in Table 1 show that the differences in the molar volume of pure components are not negligible. Because the composition in the liquid droplet and the Si/Ge ratio in the resultant $Si_{1-x}Ge_x$ nanowire would be certainly different from those in the initial bulk liquid, it is necessary to estimate the size of probable error due to the present way of estimating alloy molar volume from the initial bulk liquid composition. This could be done by conducting calculations under the same condition but using different values of molar volume and comparing the results with each other. The effect of the selected value of solid molar volume was small, as will be shown later.

The surface energy of alloys can be calculated from thermodynamic properties of the alloys and surface energy of pure elements, using Tanaka's approach [18]. Fig. 4 shows thus calculated composition dependence of surface energy in individual liquid and solid binary alloys. It should be noticed here that Ge has the lowest surface energy at the given temperature. In binary alloys containing Ge, the surface energy shows a negative deviation from the simple rule of mixture. Such negative deviation of the surface energy is accompanied by a surface segregation of the component element with lower surface energy, Ge in the present case. Because the calculation of alloy surface energy involves a numerical procedure for solving nonlinear equations, performing such calculations during phase equilibrium calculation makes the numerical procedure quite complicated. For the convenience of equilibrium calculation, some simplifications had to be made for the composition dependence of surface energy. First, the rule of mixture could be used again, assuming a linear composition dependence of the alloy surface energy. By this, the Gibbs–Thompson effect was finally expressed as follows:

$$\Delta G_{G-T} = (x_{Au}\gamma_{Au} + x_{Si}\gamma_{Si} + x_{Ge}\gamma_{Ge}) \cdot \frac{\alpha}{r} \cdot \overline{V}_m. \quad (4)$$

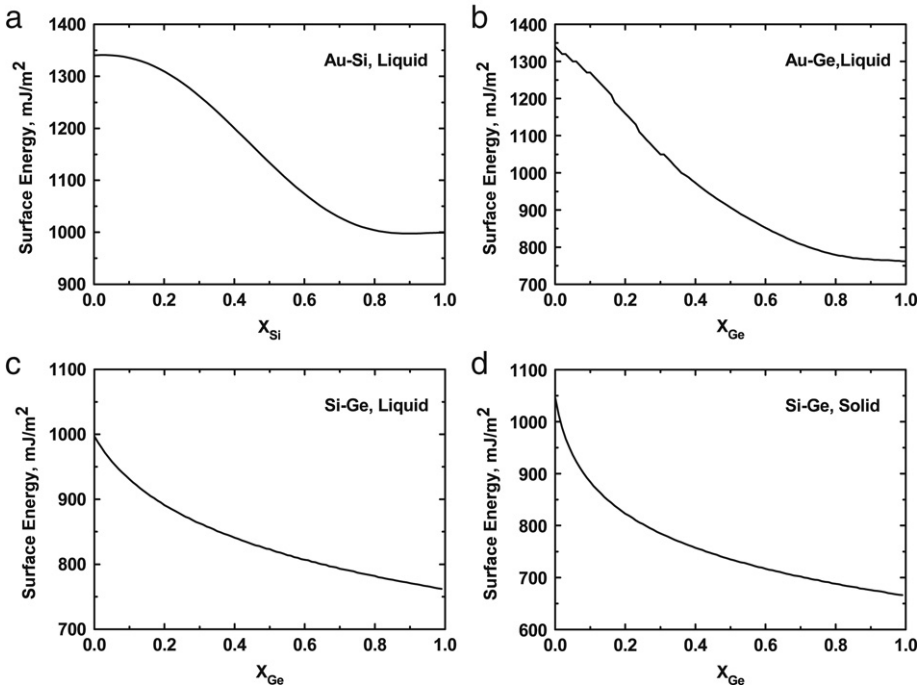

Fig. 4. Calculated surface energy in the (a) liquid Au–Si, (b) liquid Au–Ge, (c) liquid Si–Ge, and (d) solid Si–Ge alloys at 400 °C.

The calculations could be performed easily using the Thermo-Calc software by simply adding the $\frac{\alpha}{r}\gamma_i \overline{V}_m$ term for individual elements to the Gibbs energy expression of pure elements.

3. Results and discussion

Fig. 5 illustrates the final results on the size dependence of $Si_{1-x}Ge_x$ nanowire composition for the nine initial liquid compositions designated in Fig. 3. A clear size dependence (increasing Ge content with increasing wire diameter) is predicted in the whole composition range in agreement with the experiment [11]. A typical, experimentally observed size dependence of nanowire composition [11] is illustrated in Fig. 6.

All results in Fig. 5 are those obtained assuming the rule of mixture for the molar volume and surface energy of liquid and solid alloys. Further, in the case of molar volume, the estimation (application of the rule of mixture) was made based on the initial bulk liquid composition even for the solid nanowire phase. As a means to estimate the size of probable computation error that comes from the approximation made for the solid volume, calculations using different solid molar volumes were performed, and compared with original results. Instead of the average value obtained from the rule of mixture, the molar volume of pure Si or pure Ge was used for the molar volume of solid alloy. Fig. 7a shows the results for the three cases. It is shown that the effect of the selected value of solid molar volume is negligible. It is expected that similar results would be obtained for the effect of the selected value for the liquid molar volume.

As a means to estimate the probable error due to the simplification (application of the rule of mixture) made for the alloy surface energy, it was also necessary to examine the results when a different assumption was made for the alloy surface energy. The different assumption made here was to set all the alloy surface energy values (for both liquid and solid) equal to that of pure Ge. This is close to the situation where Ge atoms (the component with the lowest surface energy) are fully segregated on the liquid or solid surface. The results for this case are compared with the original ones in Fig. 7b. It is shown that the size dependence becomes slightly stronger when the surface segregation of Ge is assumed to occur completely. This is expectable because the size dependence originates from the Gibbs–Thompson effect which is proportional to the surface energy, and the substitution of γ_{Ge} for γ_{Si} would make the Si-rich side relatively more stable. It is not clear whether the surface segregation would occur to the equilibrium amount during the VLS growth of nanowires. It is expected that the real situation would correspond to somewhere between the two extreme cases in Fig. 7b.

Even though some approximations were made to estimate the molar volume and surface energy of liquid droplets and solid nanowires, the present thermodynamic analysis clearly shows that the experimentally observed size dependence of the VLS grown $Si_{1-x}Ge_x$ nanowire composition indeed originates from the capillarity effect and that those approximations made for the molar volume and surface energy does not have effect on the conclusion. An attempt will now be made to further analyze and rationalize the present results. In Fig. 8, the compositions of liquid droplets (empty squares) and resultant solid nanowires (empty triangles) are plotted in comparison with some initial bulk liquid compositions (filled squares). It is shown that the compositions of nano liquid droplets are shifted to the Au-rich side and also slightly to the Si-rich side. The compositional shifts to the Si-rich side of solid nanowires from liquid droplets are small or even the opposite when compared to those of liquid droplets from the initial bulk liquid. This means that the compositional change due to the capillarity effect occurs already in the liquid droplets rather than during the growth of solid nanowire from supersaturated liquid droplets. This does not mean that no compositional change would occur if the nanowires are grown directly from vapor without the liquid droplets. One should consider that for comparable size of surface energy and molar volume, the capillarity effect would be stronger in spherical liquid droplets where the geometrical factor α is 2 than in cylindrical solid nanowires where α is 1.

The shift of liquid droplet composition to the Au-rich side of the initial bulk composition can be easily explained by Fig. 9. It is shown schematically that the amount of supersaturation of Si or Ge is reduced in nano droplets which have higher Gibbs free energy than the bulk liquid due to the capillarity effect. In order to find

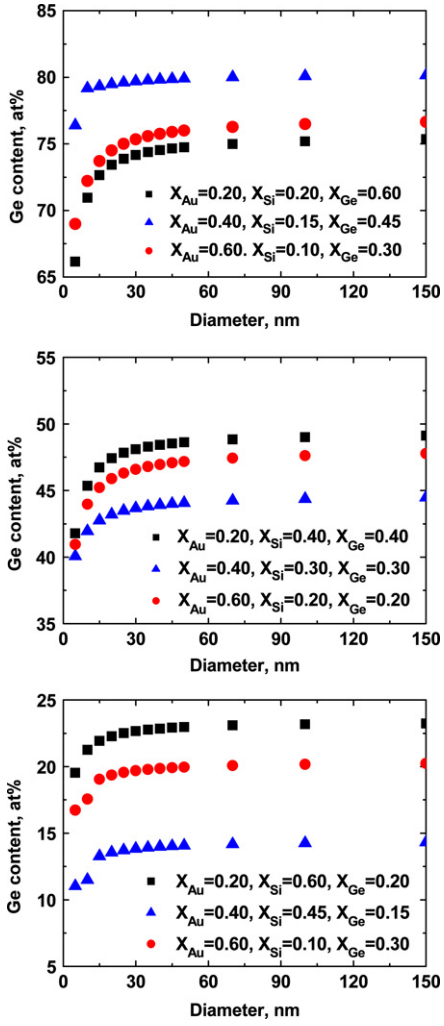

Fig. 5. Calculated size dependence of Si–Ge nanowire composition for the given initial liquid compositions designated in Fig. 3.

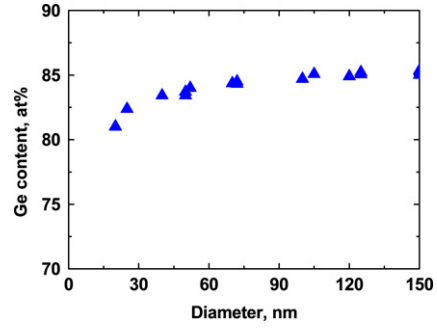

Fig. 6. A typical example of experimentally observed size dependence of Si–Ge nanowire composition, obtained at 325 °C [11].

the probable explanation for the shift of liquid droplet composition to the Si-rich side, the Gibbs free energy of formation of Au–Si and Au–Ge binary liquid alloys were calculated. The results are presented in Fig. 10. Important here is that the Gibbs energy of the Au–Si liquid decreases more rapidly with increasing Au content than the Au–Ge liquid. This means that the Au–Si binary alloys become relatively more stable than Au–Ge binary alloys as the overall composition moves toward the Au-rich side. Therefore, it can be concluded that the direct result of the capillarity effect is the shift of the liquid droplet composition to the Au-rich side,

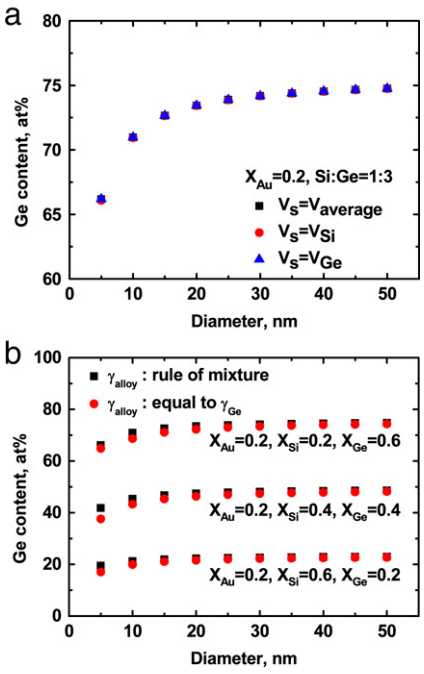

Fig. 7. Effects of selected values of (a) solid molar volume and (b) alloy surface energy on the size dependence of Si–Ge nanowire composition.

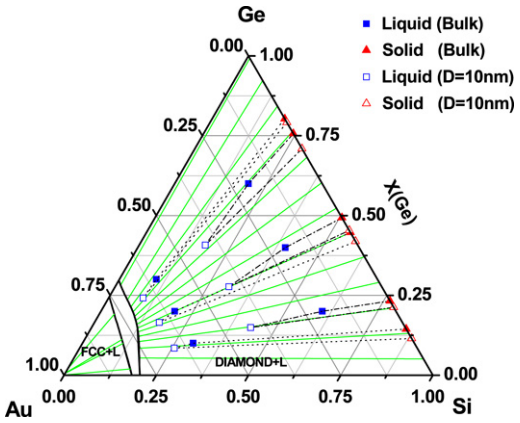

Fig. 8. The compositional change of liquid droplets (empty squares) and resultant solid nanowires (empty triangles) from the initial bulk liquid compositions (filled squares). The filled triangles represent solid compositions that would be obtained from the initial bulk liquid compositions if the capillarity effect was not considered. The phase diagram is the 400 °C isothermal section of the Au–Si–Ge ternary system.

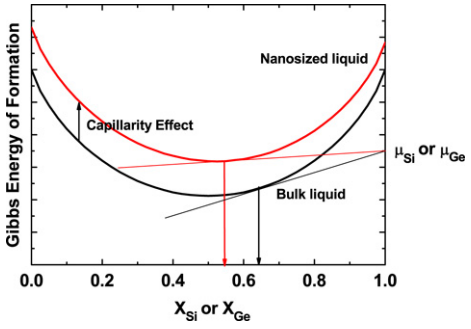

Fig. 9. Schematic illustration for the shift of equilibrium composition due to the capillarity effect.

which results in the further shift into the Si-rich side due to the thermodynamic property of the Au–Ge-Si ternary liquid alloys.

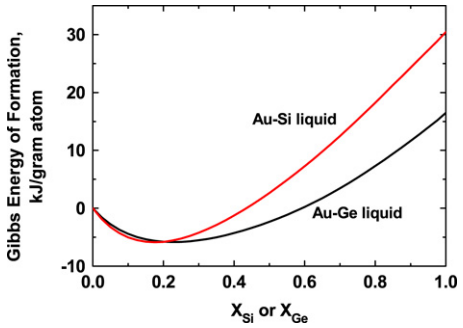

Fig. 10. Gibbs energy of formation of Au–Ge and Au–Si liquid alloys at 400 °C.

Finally, it should be mentioned that the experimentally observed size dependence of nanowire composition shown in Fig. 6 is slightly stronger than the present thermodynamic calculation shown in Fig. 5. The present authors believe that kinetic effects would also have to be considered as well as the thermodynamic effect, as was done in [22,23] to explain the reason for the growth of nanowires below the eutectic temperature. As has been done in many kinetic studies on materials phenomena, the thermodynamic analysis as given in the present work can be a start point for more sophisticated studies.

4. Conclusion

We have shown that the size dependence of the VLS grown $Si_{1-x}Ge_x$ nanowire composition originates from the capillarity effect. It was also shown that the direct result of the capillarity effect is the shift of the liquid droplet composition to the Au-rich side, which results in the further shift into the Si-rich side due to the thermodynamic property of the Au–Ge-Si ternary liquid alloys. Because of the unknown incorporation rate of SiH_4 or GeH_4 on the liquid surface, it was impossible to predict the composition of nanowires quantitatively from the given process condition. However, the present thermodynamic approach can be a start point for more quantitative study to predict and control the composition of alloy nanowires synthesized by similar methods.

Acknowledgement

This work has been financially supported by the Korea Science and Engineering Foundation (KOSEF) grant funded by the Korea government (MOEST) (Grant No. R01-2006-000-10585-0).

References

[1] D.P. Yu, Q.L. Hang, Y. Ding, H.Z. Zhang, Z.G. Bai, J.J. Wang, Y.H. Zou, W. Qian, G.C. Xiong, S.Q. Feng, Appl. Phys. Lett. 73 (1998) 3076.
[2] J.Q. Hu, Y. Jiang, X.M. Meng, C.S. Lee, S.T. Lee, Chem. Phys. Lett. 367 (2003) 339.
[3] X.D. Wang, E. Graugnard, J.S. King, Z.L. Wang, C.J. Summers, Nano Lett. 4 (2004) 2223.
[4] J.W.P. Hsu, Z.R. Tian, N.C. Simmons, C.M. Matzke, J.A. Voigt, J. Liu, Nano Lett. 5 (2005) 83.
[5] X. Duan, C.M. Lieber, Adv. Mater. 12 (2000) 298.
[6] Y. Wu, R. Fan, P. Yang, Nano Lett 2 (2002) 83.
[7] N.D. Zakharov, P. Werner, G. Gerth, L. Schubert, L. Sokolov, U. Gosele, J. Cryst. Growth 290 (2006) 6.
[8] K.K. Lew, L. Pan, E.C. Dickey, J.M. Redwing, Adv. Mater. 15 (2003) 2073.
[9] K.-K. Lew, L. Pan, E.C. Dickey, J.M. Redwing, J. Mater. Res. 21 (2006) 2876.
[10] J.E. Yang, C.B. Jin, C.J. Kim, M.H. Jo, Nano Lett. 6 (2006) 2679.
[11] X. Zhang, K.K. Lew, P. Nimmatoori, J.M. Redwing, E.C. Dickey, Nano Lett. 7 (2007) 3241.
[12] E.I. Givargizov, J. Cryst. Growth 31 (1975) 20.
[13] B. Sundman, B. Jansson, J.-O. Andersson, Calphad 9 (1985) 153.
[14] SGTE solution and pure substance database http://www.sgte.org.
[15] L. Kaufman, H. Bernstein, Computer Calculations of Phase Diagrams with Special Reference to Refractory Metals, Academic Press, New York, 1970.
[16] G. Ouyang, L.H. Liang, C.X. Wang, G.W. Yang, Appl. Phys. Lett. 88 (2006) 091914_1.
[17] V.V. Zakharov, E.N. Brodskaya, A. Laaksonen, J. Chem. Phys. 107 (1997) 10675.
[18] T. Tanaka, K. Hack, T. Iida, S. Hara, Z. Metallkd 87 (1996) 380.
[19] T. Iida, R.I.L. Guthrie, The Physical Properties of Liquid Metals, Clarendon Press, Oxford, 1988.
[20] L.Z. Mezey, J. Giber, Jpn. J. Appl. Phys 21 (1982) 1569.
[21] ASM Handbooks Online. ASM Handbook Volume 2, Properties and Selection: Nonferrous Alloys and Special-Purpose Materials, ASM International http://www.asmmaterials.info.
[22] H. Adhikari, A.F. Marshall, I.A. Goldthorpe, C.E.D. Chidsey, P.C. McIntyre, ACS Nano 1 (2007) 415.
[23] S. Kodambaka, J. Tersoff, M.C. Reuter, F.M. Ross, Science 316 (2007) 729.